

Published in final edited form as:

J Mol Biol. 2008 February 1; 375(5): 1206–1211. doi:10.1016/j.jmb.2007.11.050.

Trapping of a transcription complex using a new nucleotide analogue: AMP Aluminium Fluoride

Nicolas Joly^{1,†}, Mathieu Rappas^{2,†}, Martin Buck^{1,*}, and Xiaodong Zhang^{2,*}

¹Division of Biology, Sir Alexander Fleming Building, Imperial College London, Exhibition Road, South Kensington, London, SW7 2AZ, UK.

²Division of Molecular Biosciences, Biochemistry Building, Imperial College London, Exhibition Road, South Kensington, London, SW7 2AZ, UK.

Summary

Mechanochemical proteins rely on ATP-hydrolysis to establish the different functional states required for their biological output. Studying the transient functional intermediate states these proteins adopt as they progress through the ATP-hydrolysis cycle is key to understanding the molecular basis of their mechanism. Many of these intermediates have been successfully ‘trapped’ and functionally characterised using ATP analogues. Here, we present a new nucleotide analogue, AMP-AIF_x, which ‘traps’ PspF, a bacterial Enhancer Binding Protein, in a stable complex with the σ^{54} -RNA polymerase holoenzyme. The crystal structure of AMP-AIF_x•PspF₁₋₂₇₅ provides new information on protein-nucleotide interactions and suggests that the β and γ phosphates are more important than the α phosphate in terms of sensing nucleotide bound states. In addition, functional data obtained with AMP-AIF_x establish distinct roles for the conserved catalytic AAA⁺ residues suggesting that AMP-AIF_x is a powerful new tool to study AAA⁺ protein family members and more generally Walker motif ATPases.

Keywords

AAA⁺ ATPase; nucleotide analogue; transcription; bEBP; PspF

In bacteria, the major variant sigma factor, sigma54 (σ^{54}), forms a transcriptionally silent closed complex (CC) with RNA polymerase (E) at σ^{54} -dependent promoters. ATP-hydrolysis by a σ^{54} activator protein that belongs to the large AAA⁺ (ATPases Associated with various cellular Activities) protein family is required to actively remodel the CC to a transcriptionally competent open complex (OC) 1; 2; 3. σ^{54} -activators are also termed bacterial Enhancer Binding Proteins (bEBP; 4) as they often bind Upstream Activating Sequences (UAS) located approximately 100 bp upstream from the σ^{54} promoter. bEBP, like most AAA⁺ proteins, first need to oligomerise (usually to form hexamers) to be functionally active. What distinguishes bEBPs from other AAA⁺ family members is the presence of a highly conserved GAFTGA motif, shown to be essential for σ^{54} binding, found at the tip of the L1 loop 5; 6; 7; 8; 9. Structurally characterised bEBPs include NtrC1, PspF, ZraR and NtrC 7; 8; 9; 10. The AAA⁺ domains of NtrC1 and PspF form functionally relevant stable complexes with σ^{54} or σ^{54} in the presence of the nucleotide analogues ADP-BeF_x and ADP-AIF_x thought to mimic the ATP-bound state prior to, or at the point of, ATP-hydrolysis, respectively 8; 11; 12; 13. The complexes formed using these nucleotide

* Corresponding authors. Tel: +44 (0) 2075945442, Fax: +44 (0) 2075945419. m.buck@imperial.ac.uk, xiaodong.zhang@imperial.ac.uk.

[†]N.J. and M.R. contributed equally to this work.

analogues have been proposed to closely represent otherwise transient intermediates formed with ATP. However, the precise number and arrangement of the fluoride ions in the AlF_x or BeF_x moieties within the nucleotide-binding pockets of these bEBPs remains unknown, making the exact assignment of the respective complexes to the different nucleotide states (ground or transition state) somewhat uncertain. We previously proposed that sensing the nucleotide-bound state of PspF involves the Walker B residue E108 and that via its interaction with residue N64 the ATP can affect the conformation of the σ^{54} interacting L1 loop 14. We proposed that in the ADP-bound state the L1 loop is locked in a non-productive conformation, unable to interact with σ^{54} . Upon ATP binding, an interaction between E108 and N64 promotes the release of the L1 loop, enabling the interaction with σ^{54} to take place 12; 14. At the point of ATP-hydrolysis, the L1 loop is further exposed allowing more stable interactions with σ^{54} to occur.

Nucleotide analogues are routinely used to capture proteins in transient conformational states; they are thus indispensable tools to successfully study and dissect the different stages of nucleotide hydrolysis driven molecular mechanisms. Here, we report the identification and functional characterisation of a new stable complex between the AAA^+ domain of PspF (residues 1 to 275, called hereafter PspF₁₋₂₇₅) and σ^{54} or $\text{E}\sigma^{54}$ using the new nucleotide analogue AMP- AlF_x formed *in situ*. In addition, using site-directed mutagenesis and biochemical approaches, we assign the residues in PspF₁₋₂₇₅ that are responsible for forming either the ADP- AlF_x - or the AMP- AlF_x -dependent complexes. Detailed analysis of our data suggests that the highly conserved AAA^+ catalytic residues, including the Walker B motif residues and the putative arginine finger (R-finger) residues, have distinct roles in catalysis and may therefore be implicated in PspF functionality at different stages of the hydrolysis cycle.

AMP- AlF_x complex formation

To investigate whether nucleotide analogues other than ADP- AlF_x support formation of stable complexes between the activator protein and σ^{54} or $\text{E}\sigma^{54}$, we performed “trapping experiments” as described by 11; 15, in which we replaced ADP with AMP. Incubation of PspF₁₋₂₇₅ Wild Type (WT) with σ^{54} or $\text{E}\sigma^{54}$ in the presence of AMP, AlCl_3 and NaF lead to formation of stable AMP- AlF_x •PspF₁₋₂₇₅WT• σ^{54} or AMP- AlF_x •PspF₁₋₂₇₅• $\text{E}\sigma^{54}$ complexes which migrate with the same mobility as ADP- AlF_x dependent complexes on native gels suggesting that they are very similar (Figure 1A lanes 2, 3, 8 and 9). As a control, we demonstrated that AMP alone did not support formation of stable complexes between PspF₁₋₂₇₅ and σ^{54} (or $\text{E}\sigma^{54}$) (Figure 1A lanes 4-6). Interestingly, we noted that when using the histidine-tagged form of PspF₁₋₂₇₅WT [(His)₆-PspF₁₋₂₇₅WT] we observed a stable homo-hexameric of (His)₆-PspF₁₋₂₇₅WT in the presence of ADP- AlF_x but not AMP- AlF_x , suggesting differences between PspF₁₋₂₇₅WT subunits exist in the presence of these two nucleotide analogues (Table 1).

AMP- AlF_x trapped complex characterisation

To further characterise the new AMP- AlF_x •PspF₁₋₂₇₅• σ^{54} (or $\text{E}\sigma^{54}$) complex, we performed gel filtration experiments. Elution profiles of the PspF₁₋₂₇₅• σ^{54} complexes obtained using either ADP- AlF_x - or AMP- AlF_x are very similar (Figure 1B). We thus conclude from the gel filtration and band shift assays that the ADP- AlF_x - and AMP- AlF_x -dependent complexes are similar in terms of size and stability. In addition, DNA binding assays, using fluorescent probes mimicking different promoter DNA conformations 16, demonstrated no significant differences in the DNA binding properties of the two types of ‘trapped’ complexes (data not shown). Having established that the AMP- AlF_x -dependent complexes can bind DNA, we investigated whether the AMP- AlF_x •PspF₁₋₂₇₅• $\text{E}\sigma^{54}$ complex was able to activate

transcription *in vitro* from the supercoiled *S. meliloti nifH* promoter. Similar to the ADP-AIF_x•PspF₁₋₂₇₅•Eσ⁵⁴ complex, transcription from the AMP-AIF_x•PspF₁₋₂₇₅•Eσ⁵⁴ complex was not observed (data not shown). Finally, using in-solution DNA crosslinking (as described in 17) we found no significant differences between the ADP-AIF_x- and AMP-AIF_x-dependent complexes formed with σ⁵⁴, suggesting that the protein•DNA interactions are similar when using the two AIF_x dependent nucleotide analogues (P. Burrows and N. Joly, unpublished result).

Taken together, these results indicate that both AMP-AIF_x- and ADP-AIF_x-dependent complexes are likely to have similar conformations and stability although some subtle differences do exist.

Structure of Mg-AMP bound PspF₁₋₂₇₅

To establish the detailed organisation of Mg-AMP-AIF_x-bound PspF₁₋₂₇₅, and to provide a structural basis for the distinct determinants implicated in forming ADP-AIF_x versus AMP-AIF_x complexes, we soaked PspF₁₋₂₇₅ crystals with MgCl₂, AMP, AlCl₃ and NaF (Table 2). These crystals diffracted to 2.85 Å at ESRF and the structure was solved by molecular replacement using the structure of apo PspF₁₋₂₇₅ WT as a search model. Inspection of the first FoFc map contoured at 3 sigma (3σ), revealed clear densities for both the AMP and the Mg moieties and an extra density located at the tip of the α-phosphate of the AMP moiety (Figure 2A), which is too large to be a water molecule. We believe this density corresponds to the AIF_x moiety but because of the low resolution we cannot establish this unambiguously and are thus unable to conclude anything regarding the precise coordination of the Al ion. The structure however clearly shows that the torsion angles around the ribose moiety and the phosphate backbone have significantly changed when compared with those in either the AMPPNP-, ATP- or ADP-bound structures 14. The torsion angle of the C₄'-C₅' bond changes 114°, from 38° in the ATP-bound structure to 152° in the Mg-AMP-bound structure and as a result the ribose plane is translated some 3 Å towards the Walker B motif allowing the α-phosphate of AMP to occupy the canonical position of the β-phosphate of ATP (Figure 2). The extra electron density (potentially the AIF_x moiety) occupies a similar position to that of the γ-phosphate of ATP in the ATP-bound structure (Figure 2; 14). We also observe a water molecule sitting where the apical oxygen (O) of the α-phosphate of ATP lies in the ATP-bound structure (Figure 2; 14). Interestingly, the N-terminus of PspF appears more structured and has moved 0.5 Å towards the Walker B motif when compared to the ATP-bound structure. This movement of the N-terminus could promote or facilitate the translation of AMP to compensate for the missing β-phosphate.

When superposing the ATP-bound structure onto the Mg-AMP-bound structure, ATP fits convincingly into the FoFc difference map contoured at 3σ (Figure 2B). We note that the α-phosphate of ATP lies outside the density whereas the β-phosphate and γ-phosphate fit inside it. This observation suggests that the AMP-AIF_x analogue, regardless of the coordination of the Al, mimics more closely a tri-phosphate nucleoside rather than a di-phosphate one. Furthermore, when comparing the Mg-AMP-bound structure to the AMPPNP-, Mg-ATP- and ADP-bound structures 14 we notice that certain key residues and secondary structure elements adopt conformations that are closer to those previously observed in the tri-phosphate nucleoside bound structures. Indeed, the crucial Walker B E108 residue adopts in the Mg-AMP-bound structure a conformation midway between that observed in the AMPPNP-bound structure and that observed in the Mg-ATP-bound structure. Also, the L1 loop in the Mg-AMP-bound structure is as ordered and points in the same direction as in the AMPPNP-bound structure. L1 loop is not as disordered as in the Mg-ATP-bound structure and it points up instead of pointing down as it does in the ADP-bound structure. Finally, in the Mg-AMP-bound structure the N-terminus of PspF appears

more structured and has moved 0.5 Å towards the Walker B motif when compared to the N-terminus in the Mg-ATP-bound structure and 1.2 Å when compared to the ADP-bound structure. This movement of the N-terminus could promote or facilitate the translation of the AMP to compensate for the missing β-phosphate.

Translation of the AMP is consistent with results using the human Guanylate Binding Protein 1 (hGBP1), which showed a clear di-phosphatase activity and revealed that GMP-AIF₄ adopts a conformation that permits the AIF₄ moiety to occupy the canonical position of the γ-phosphate of GTP 18. Interestingly, for hydrolysis of GDP to occur, the GDP moiety has to be translated in the binding pocket, and the torsion angle between the ribose moiety and the phosphate backbone needs to change so that the β-phosphate of GDP occupies the canonical position of the γ-phosphate of GTP whilst the α-phosphate occupies that of the β-phosphate, similar to the Mg-AMP-bound structure presented here (Figure 2). We did not detect hydrolysis of ATP (or ADP) to AMP by PspF₁₋₂₇₅.

Determinants for ADP-AIF_x versus AMP-AIF_x complex formation

In order to better understand the organisation of AMP and ADP within AIF_x-containing complexes, and to probe any intrinsic differences between these two complexes, we chose to mutate residues implicated in ATP binding and hydrolysis. More specifically, residues that contact the γ-phosphate and the β-phosphate of ATP, as well as the potential ‘trans’ (provided by the neighbouring subunit) R-finger residues involved in inter-subunit ATP-hydrolysis were substituted using site-directed mutagenesis. Using the same experimental approach as described in Figure 1A, we screened for complexes formed with PspF₁₋₂₇₅ variants. Two distinct classes of residues emerged: (i) residues required for forming both ADP-AIF_x and AMP-AIF_x-dependent complexes; and (ii) residues essential only for AMP-AIF_x-dependent complex formation.

Residues implicated in both ADP-AIF_x- and AMP-AIF_x-dependent complex formation include the Walker A residue K42, the ribose interacting residue L44, the Walker B residue E108 and the ‘trans’ R-finger residue R168 (‘R168’) (Table 1). Substitution of these residues with alanine eliminated both ADP-AIF_x- and AMP-AIF_x-dependent complex formation. Specific determinants for AMP-AIF_x complex formation are the Walker B D107 residue and the ‘trans’ R-finger residue R162 (‘R162’) (Table 1).

The Walker B motif residues D107 and E108 and the R-finger residues R162 and R168 are conserved features among AAA⁺ proteins. They are categorized as catalytic residues since their substitution results in significantly reduced ATP-hydrolysis ability 19. Interestingly, the integrity of D107 is required for AMP-AIF_x-dependent complex formation, but not for ADP-AIF_x-dependent complex formation (Table 1). We infer that D107 is probably involved first in γ-phosphate coordination and then in hydrolysis *per se* 17. Mutating D107 would thus affect interaction with the γ-phosphate, but not the latter state when the β-γ phosphate bond has been cleaved, as it is no longer involved in nucleotide interaction due to the change in valence of the γ-phosphate of ATP after nucleophilic attack. Integrity of E108 is required for formation of ADP- and AMP-AIF_x dependent complexes, consistent with its role in sensing the state of the γ-phosphate (either cleaved or non-cleaved) and transmitting changes to the σ⁵⁴ interacting L1 loop 17. Mutation of E108 presumably impairs the ability to detect the γ-phosphate, hence affecting complex formation when using either AMP-AIF_x or ADP-AIF_x (Table 1). Importantly, to relay the state of the γ-phosphate in one subunit to the remaining hexameric assembly, thereby enabling hydrolysis, ‘R162’ contributes to formation of the catalytic centre in the neighbouring subunit. Since the integrity of R162 is required for AMP-AIF_x- but not ADP-AIF_x-dependent complex formation, we propose that ‘R162’ is also involved in γ-phosphate coordination and catalysis. As integrity of R168

is required for both AMP-AIF_x- and ADP-AIF_x-dependent complex formation, ¹R168 is probably involved in interactions with other parts of the nucleotide (namely the C₂' and C₃' hydroxyl groups), acting as a nucleotide-dependent self-association determinant rather than a catalytic residue *per se* 14. It is interesting to note that we were unable to identify a mutation which supports formation of a stable AMP-AIF_x complex and not an ADP-AIF_x complex.

In this study, we identified and characterised a new nucleotide analogue supporting formation of a stable bEBP•σ⁵⁴ (Eσ⁵⁴) complex. In the crystal structure of PspF₁₋₂₇₅•AMP-AIF_x we observe an extra density (probably due to the AIF_x moiety) linked to the AMP moiety, which occupies the same position as the γ-phosphate in the PspF₁₋₂₇₅-ATP-bound structure. Furthermore, in the Mg-AMP-bound structure presented here, the α-phosphate (of AMP) occupies the same position as the β-phosphate of ATP in the PspF₁₋₂₇₅-ATP-bound structure. These data taken together suggest that occupancy of the α-phosphate position is not as important as occupancy of the β-phosphate and γ-phosphate positions for stimulating stable complex formation. The change in the ribose-phosphate bond observed for AMP (compared to AMPPNP, ATP and ADP) resembles that observed for hGBP1 suggesting a level of conservation between nucleotide binding pocket properties. We propose that AMP-AIF_x will be a useful tool to study the ATP binding pockets of AAA⁺ proteins and more specifically to demonstrate how residues of the AAA⁺ catalytic centre are implicated in nucleotide stabilisation and utilisation. The apparent adaptability of AMP in this complex suggests that AMP-AIF_x could enable identification of new functional states of AAA⁺ proteins in complex with their natural target. Finally, to our knowledge, this is the first time that AMP-AIF_x has been reported to act as a nucleotide analogue. It can therefore be regarded as a powerful new tool to study the mechanisms of other AAA⁺ protein family members and more generally Walker motif ATPases.

Supplementary Material

Refer to Web version on PubMed Central for supplementary material.

Acknowledgments

We thank Dr P. Burrows for comments on the manuscript. We are grateful to members of Prof. Buck's and Dr Zhang's labs for helpful discussions and friendly support. This work was supported by grants from the BBSRC and Wellcome Trust to M.B. and X.Z. M.B. acknowledges fellowship support from the Leverhulm trust. N.J. was the recipient of an EMBO fellowship (ALTF 387-2005).

References

1. Rappas M, Bose D, Zhang X. Bacterial enhancer-binding proteins: unlocking sigma(54)-dependent gene transcription. *Curr Opin Struct Biol.* 2007; 17:110–6. [PubMed: 17157497]
2. Schumacher J, Joly N, Rappas M, Zhang X, Buck M. Structures and organisation of AAA+ enhancer binding proteins in transcriptional activation. *J Struct Biol.* 2006
3. Wigneshweraraj SR, Burrows PC, Bordes P, Schumacher J, Rappas M, Finn RD, Cannon WV, Zhang X, Buck M. The second paradigm for activation of transcription. *Prog Nucleic Acid Res Mol Biol.* 2005; 79:339–69. [PubMed: 16096032]
4. Wedel A, Weiss DS, Popham D, Droge P, Kustu S. A bacterial enhancer functions to tether a transcriptional activator near a promoter. *Science.* 1990; 248:486–90. [PubMed: 1970441]
5. Bordes P, Wigneshweraraj SR, Chaney M, Dago AE, Morett E, Buck M. Communication between Esigma(54), promoter DNA and the conserved threonine residue in the GAFTGA motif of the PspF sigma-dependent activator during transcription activation. *Mol Microbiol.* 2004; 54:489–506. [PubMed: 15469519]

6. Bordes P, Wigneshweraraj SR, Schumacher J, Zhang X, Chaney M, Buck M. The ATP hydrolyzing transcription activator phage shock protein F of *Escherichia coli*: identifying a surface that binds sigma 54. *Proc Natl Acad Sci U S A*. 2003; 100:2278–83. [PubMed: 12601152]
7. Lee SY, De La Torre A, Yan D, Kustu S, Nixon BT, Wemmer DE. Regulation of the transcriptional activator NtrC1: structural studies of the regulatory and AAA+ ATPase domains. *Genes Dev*. 2003; 17:2552–63. [PubMed: 14561776]
8. Rappas M, Schumacher J, Beuron F, Niwa H, Bordes P, Wigneshweraraj S, Keetch CA, Robinson CV, Buck M, Zhang X. Structural insights into the activity of enhancer-binding proteins. *Science*. 2005; 307:1972–5. [PubMed: 15790859]
9. Sallai L, Tucker PA. Crystal structure of the central and C-terminal domain of the sigma(54)-activator ZraR. *J Struct Biol*. 2005; 151:160–70. [PubMed: 16005641]
10. De Carlo S, Chen B, Hoover TR, Kondrashkina E, Nogales E, Nixon BT. The structural basis for regulated assembly and function of the transcriptional activator NtrC. *Genes Dev*. 2006; 20:1485–95. [PubMed: 16751184]
11. Chaney M, Grande R, Wigneshweraraj SR, Cannon W, Casaz P, Gallegos MT, Schumacher J, Jones S, Elderkin S, Dago AE, Morett E, Buck M. Binding of transcriptional activators to sigma 54 in the presence of the transition state analog ADP-aluminum fluoride: insights into activator mechanochemical action. *Genes Dev*. 2001; 15:2282–94. [PubMed: 11544185]
12. Chen B, Doucleff M, Wemmer DE, De Carlo S, Huang HH, Nogales E, Hoover TR, Kondrashkina E, Guo L, Nixon B.T. ATP Ground- and Transition States of Bacterial Enhancer Binding AAA+ ATPases Support Complex Formation with Their Target Protein, sigma54. *Structure*. 2007; 15:429–440. [PubMed: 17437715]
13. Wittinghofer A. Signaling mechanistics: aluminum fluoride for molecule of the year. *Curr Biol*. 1997; 7:R682–5. [PubMed: 9382787]
14. Rappas M, Schumacher J, Niwa H, Buck M, Zhang X. Structural basis of the nucleotide driven conformational changes in the AAA+ domain of transcription activator PspF. *J Mol Biol*. 2006; 357:481–92. [PubMed: 16430918]
15. Joly N, Schumacher J, Buck M. Heterogeneous nucleotide occupancy stimulates functionality of phage shock protein F, an AAA+ transcriptional activator. *J Biol Chem*. 2006; 281:34997–5007. [PubMed: 16973614]
16. Cannon W, Bordes P, Wigneshweraraj SR, Buck M. Nucleotide-dependent triggering of RNA polymerase-DNA interactions by an AAA regulator of transcription. *J Biol Chem*. 2003; 278:19815–25. [PubMed: 12649285]
17. Joly N, Rappas M, Wigneshweraraj SR, Zhang X, Buck M. Coupling nucleotide hydrolysis to transcription activation performance in a bacterial enhancer binding protein. *Mol Microbiol*. 2007; 66:583–595. [PubMed: 17883390]
18. Ghosh A, Praefcke GJ, Renault L, Wittinghofer A, Herrmann C. How guanylate-binding proteins achieve assembly-stimulated processive cleavage of GTP to GMP. *Nature*. 2006; 440:101–4. [PubMed: 16511497]
19. Hanson PI, Whiteheart SW. AAA+ proteins: have engine, will work. *Nat Rev Mol Cell Biol*. 2005; 6:519–29. [PubMed: 16072036]
20. Emsley P, Cowtan K. Coot: model-building tools for molecular graphics. *Acta Crystallogr D Biol Crystallogr*. 2004; 60:2126–32. [PubMed: 15572765]

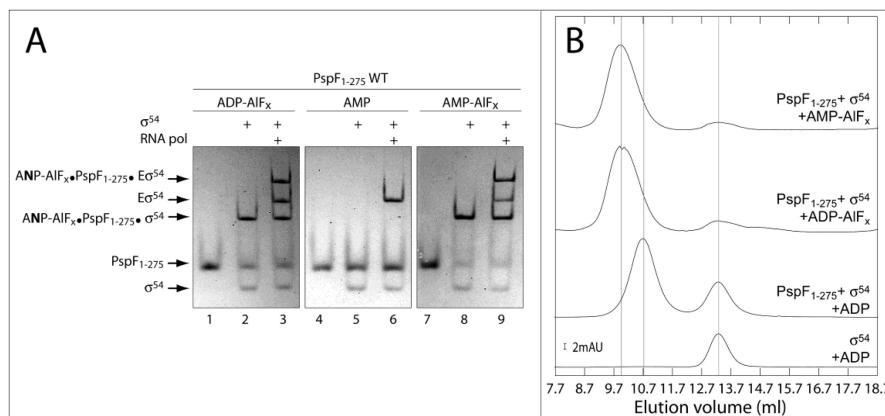


Figure 1. Identification and characterisation of new stable PspF₁₋₂₇₅ WT·σ⁵⁴ or Eσ⁵⁴ complexes in the presence of AMP-AIF_x

A- Native gel showing the complexes formed by PspF₁₋₂₇₅ WT (5 μM) ± σ⁵⁴ (1 μM) ± RNA polymerase (0.15 μM) in the presence of AIF_x reactant (AlCl₃ (0.4 mM) + NaF (5 mM)) and different nucleotides (4 mM, as indicated). The sample was loaded onto native PAGE 4.5% and proteins were detected by Coomassie Blue staining. ANP indicates AMP or ADP.

B- Gel filtration profiles of samples containing PspF₁₋₂₇₅ WT (64 μM) ± σ⁵⁴ (30 μM) ± AMP-AIF_x or ADP-AIF_x (as indicated) chromatographed through a Superdex 200 column (10×300 mm, 24 ml, GE Healthcare) at 4 °C. The *scale bars* give the scale of the ordinate axis; absorbation units (AU) correspond to an A_{280nm} of 1.

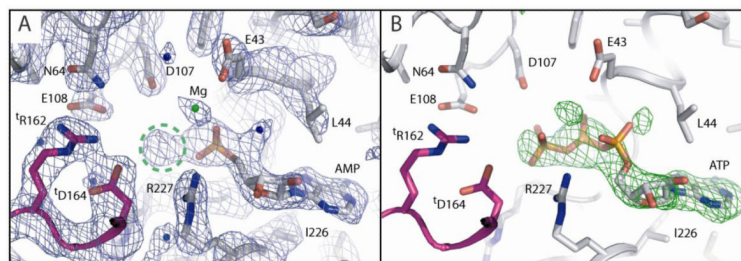


Figure 2. Final $2F_oF_c$ and omit difference F_oF_c electron density maps of the nucleotide binding pocket of PspF₁₋₂₇₅

A- Final $2F_oF_c$ map of the Mg-AMP-PspF₁₋₂₇₅ structure at 2.85 Å resolution contoured at 1σ . The neighbouring subunit is coloured blue. Important intra-molecular catalytic residues are highlighted and important inter-molecular catalytic residues offered by the neighbouring subunit are denoted “t” for “trans”. Note how the extra electron density encircled in green dashed lines occupies the position of the γ -phosphate in ATP-bound structures of PspF₁₋₂₇₅ and is connected to the electron density of the AMP moiety.

B- Omit difference F_oF_c map of the Mg-AMP-PspF₁₋₂₇₅ structure contoured at 3σ . The PspF₁₋₂₇₅-ATP-bound structure was superimposed onto the P-loop of the PspF₁₋₂₇₅-Mg-AMP-bound structure and the result is displayed in this figure. Note that ATP fits convincingly into the difference map. Further note how the γ -phosphate of ATP fits into the extra density encircled in figure 2A.

Data was collect at ESRF beamline ID-29. Refinement of the structure was performed as described 14 and the nucleotide and the Mg ion were refined with unit occupancy. Map inspection, model building and water molecule picking were done using Coot 20. The average temperature factors in this structure are: for the protein: 30, for the AMP: 60 and for the Mg: 57. For analysis, all the liganded (ATP: 2C96; ADP: 2C98; AMPPNP: 2C99; Mg-ATP-PspF₁₋₂₇₅R227A: 2C9C) and unliganded (Apo: 2BJW) PspF structures were aligned onto their P-loops (residues 35 to 43). All figures were prepared using Pymol (Delano, W.L. The PyMOL Molecular Graphics System (2002) on World Wide Web <http://www.pymol.org>).

Table 1

Summary of the native gel analysis demonstrating whether “trapped” complexes were obtained using PspF₁₋₂₇₅ variants and different nucleotides in the presence of AlCl₃ and NaF.

PspF ₁₋₂₇₅	Nucleotide + AlCl ₃ + NaF	alone	σ^{54}	$E\sigma^{54}$
His-WT	ADP	+	+	+
	ATP	+	+	+
	AMPPNP	-	-	-
	AMP	-	+	+
WT	ADP	-	+	+
	ATP	-	+	+
	AMPPNP	-	-	-
	AMP	-	+	+
K42A	ADP	-	-	-
	ATP	-	-	-
	AMPPNP	-	-	-
	AMP	-	-	-
L44A	ADP	-	-	-
	ATP	-	-	-
	AMPPNP	-	-	-
	AMP	-	-	-
D107A	ADP	-	+	+
	ATP	-	-	-
	AMPPNP	-	-	-
	AMP	-	-	-
E108A	ADP	-	-	-
	ATP	-	+	+
	AMPPNP	-	-	-
	AMP	-	-	-
R162A	ADP	-	+	+
	ATP	-	-	-
	AMPPNP	-	-	-
	AMP	-	-	-
R168A	ADP	-	-	-
	ATP	-	-	-
	AMPPNP	-	-	-
	AMP	-	-	-

“-” no complex observed on native gel.

“+” complex observed on native gel.

“+*” complex observed on native gel but not dependent on $AlCl_3$ + NaF 17.

Table 2Crystallographic Data and Refinement Statistics of Mg-AMP-bound PspF₁₋₂₇₅.

Structure	Mg-AMP-PspF ₁₋₂₇₅
Space group	P6 ₅
Unit Cell (Å)	a = b = 113.6; c = 39.3; $\alpha = \beta = 90^\circ$; $\gamma = 120$
A. Data reduction statistics	
λ (Å)	0.97570
Resolution (Å)	98.39-2.85 (3.0-2.85)
Unique reflections	6998
Redundancy	10.4 (10.7)
I/ σ	4.7 (1.9)
Mean ((I)/sd(I))	18.2 (6.5)
Completeness (%)	100 (100)
R _{meas} (%)	14.3 (38.3)
R _{pim} (%)	4.4 (11.6)
R _{sym} (%)	13.6 (36.4)
B. Refinement Statistics	
Reflections (work/free)	6985/348
Number of atoms	2093 (114 water molecules)
R _{work} (%)	18.6
R _{free} (%)	24.1
Ramachandran plot (%)	
Favoured regions	90.1
Additional allowed regions	9.4
Generously allowed regions	0.5
Disallowed	0
RMS Deviation from ideality	
Bond lengths (Å)	0.013
Bond angles (°)	1.4